

Super-pixel and Neighborhood Based Contour Detection

Devshri Swami and Bahrti Chaurasia

Scope College of Engineering, Bhopal, M. P., INDIA.

(Received on: June 8, Accepted: June 17, 2017)

ABSTRACT

This paper proposes an increased modularity created contour detection algorithm based on super-pixel and neighborhood pixels. Given an over segmented image that entails of many small regions, our algorithm automatically combines those neighboring regions that produce the largest increase in modularity index. When the modularity of the segmented image is increased, the method stops merging and produces the final segmented image based on super-pixel and neighborhood region pixels. To preserve the repetitive patterns in a homogeneous region, we propose a feature on the basis of the histogram of states of image gradients and use it together with the color feature to characterize the similarity of two regions. By building the similarity matrix in an adaptive manner, the over segmentation problem can be successfully avoided.

Keywords: Clustering, community detection, image Contouring, modularity, contour detection.

1. INTRODUCTION

As a very important step for these high-level image analysis tasks, image segmentation is an initial step in processing group image pixels into some sizable homogeneous regions so that the complexity of further analysis can be substantially reduced. Image segmentation has received considerable attention since the problem was proposed¹⁻⁸, yet it still remains to be a challenging problem because of the following reasons: 1) image segmentation is an ill-defined problem and the optimal segmentation is user or application dependent and 2) image segmentation is time consuming in that each image includes a large number of pixels, especially for high-resolution images, and this prevents image segmentation from being applied to real-time applications. In fact, Gestalt principles⁹ and some cognition and psychological studies¹⁰ have noted that several key factors affect perceptual grouping a lot; for example, proximity, similarity, regularity, that is, the repetitive patterns, relative size, and so on. In this paper, we will consider all these factors and develop a computational efficient algorithm. Moreover, comprehensive evaluations of the segmentation performance under various metrics are also presented.

The mean shift algorithm³ treats image segmentation as a problem of clustering by detecting the modes of the probability density function in the feature space. Each pixel in the image is transformed to the joint spatial-range feature space by concatenating the pixel color value and its spatial coordinates into a single vector. Then the mean shift procedure is applied in this feature space to yield a convergence point for each pixel. All the pixels whose convergence points are closer than the spatial bandwidth h_r and the range bandwidth h_r are claimed to be in the same segment. In addition, minimum segment size is enforced to guarantee sizable segmentation. Although this method is usually fast, it is very sensitive to the bandwidth parameter h_r and h_s , and often results in over segmentation. Because it is based on the density estimation of the color feature for all the pixels, some smooth changes in brightness and texture or the regularities of different colors will converge to different modes, though they belong to the same segment visually. For each iteration, the algorithm merges component C1 and C2 connected by the current edge, if the corresponding edge weight is less than

$$\min(\text{Int}(C1) + \tau(C1), \text{Int}(C2) + \tau(C2)) \quad (1)$$

Where $\text{Int}(C)$ is the internal difference of component C, defined as the largest weight in the minimum spanning tree of component C, $\tau(C) = k/|C|$, and k is a constant parameter to control the minimized size of the segment. This algorithm gives nearly linear time complexity; however, it is very difficult to tune the parameter k for optimal segmentation. Normalized cut², as another popular graph partition based approach, incorporates the global information of the image into the segmentation process by studying the spectral characteristics of the graph. Given an affinity matrix W with each entry representing the similarity of two pixels, normalized cut tries to solve the generalized eigenvector problem

$$(D - W)y = \lambda Dy \quad (2)$$

Where D is the diagonal matrix with its diagonal entry $d_{ii} = \sum_j W_{ij}$. Then the segmentation is achieved by clustering the eigenvectors. Because of the high computational cost, it can only deal with images of relatively small size. A variant is the multiscale normalized cut approach¹¹, which allows us to deal with larger images by compressing large images into multiple scales. However, it has the same problem with normalized cut, specifically, it: 1) often breaks uniform or smooth regions where the eigenvectors have smooth gradients; 2) has a high time complexity; and 3) needs a predefined number of segments, which itself is a challenging problem to deal with. More graph-based segmentation can be found in¹²⁻¹⁴. However, they all need human intervention, that is, they need a user to specify the number of regions resulting from image segmentation.

The Watershed segmentation method regards the gradient magnitude of an image as a topographic surface. The pixels where a water drop starts from would drain to the same local intensity minimum are in one segment, which is called catchment basins. The lines separating the catchment basins are the watersheds, namely, the boundaries. Various improved methods are available¹⁵⁻¹⁸, but these methods are generally sensitive to noise and easily lead to over segmentation. The compression-based texture merging (CTM) method¹⁹ fits the image textures by using the Gaussian mixture model, and employs the principle of minimum description

length to find the optimal segmentation, which gives the minimum coding length under a certain distortion ratio. Later, the texture and boundary encoding-based segmentation algorithm⁶ improves the CTM by considering a hierarchy of multiple window sizes and offering more precise coding length computation. To be specific, it only encodes the texture information inside the non overlapping windows in each region and also encodes the boundary with the adaptive chain code.

However, this greatly increases the computational time cost; besides, the texture feature used in these two algorithms is essentially the pure color information from the cutoff windows and neglects the regularities inside the image²⁰⁻²⁸, thus it may split the object with some regularities of different color. Zhang, *et al.*²⁹ worked on the estimation of bias field and segmentation of images with intensity inhomogeneity. It combines information of the neighboring pixels belonging to the same class, which makes it robust to noise^{29,30}. The combination of information from the neighboring pixels belonging to the same class, with a strong capability to separate the desired object from its background. Wang *et al.*³¹ gradually improved the constraint-based image segmentation methods, including HBC-SEG, BCIPSL, and HBC-XXSL, and shape characteristics of man-made objects. Dev *et al.*³² presented a color spaces and components, based approach using PLS-based regression for the segmentation of ground-based sky/cloud images.

The proposed method provides the suitable solution for the image object segmentation. The proposed method forms the super-pixels to clear the object and background. The neighboring region aggregation is done to improve the modularity of the region. Then feature similarity based contouring is plotted for the segmentation. The rest of the paper is organized as follows. Section 2 contains the algorithm description. Section 3 has the experimentation results. Section 4 provides the conclusion for the paper.

2. ALGORITHM DESCRIPTION

Image segmentation is connected to community detection to some level. Comparable to nodes in the same community, the pixels inside the same segment as well share some properties in common, similar to pixel color value. The alterations between image segmentation and community detection can be revealed from the following aspects: 1) different from single node in a community, single pixel cannot capture these regularities in each visually homogeneous segment; 2) the pixels within the same segment possibly have completely different properties, like color; whereas for communities, a community is a group of nodes sharing exactly similar properties.

Take the face image as a trial; the full face should be treated as one segment for the purpose of image segmentation. In contrast, for community finding, the eye pixels would be served as a discrete community, while other parts of the face would be served as another community, because the pixel color value property of the eyes is totally dissimilar from that of supplementary parts of the face; 3) compared with communities, images share some a priori information, say, nearby regions are more likely to belong to the same segment; and 4) as the aggregation process goes on, more pixels are contained within one region and the texture

inside the region keeps updating, but the properties of the collected communities do not change much. The algorithm begins from a set of over-segmented regions, thus, runs very fast, and produces sizable segmentation with the regularities inside the same object unspoiled. The overview of the proposed segmentation algorithm is summarized in Algorithm 1. And the detailed presentation of some technical points for our algorithm is as follows.

A. Superpixels

The agglomerative algorithm can start the aggregation process by treating each single pixel as a community; however, it turns out that this will be too much time consuming, especially for the first Louvain iteration. Fortunately, this is indeed not necessary, because no texture information is included for single pixel. Therefore, instead, we start with superpixels, which can reduce the computational cost as well as capture the regularities. Superpixels are a set of very small and standardized regions of pixels. Initializing with superpixels can greatly reduce the time complexity without affecting the segmentation performance. Hence, we first employ a preprocessing step to over-segment the image into a set of superpixels. This preprocessing step can be accomplished by simple K-means bunching algorithm (K is set to be a comparative large value, e.g., 200 or more) or other superpixels creating algorithms. In our implementation, we use a publicly available code³¹ to get the superpixel initialization. The superpixel generation step usually gives more than 200 over-segmented regions on average. This step can greatly reduce the complexity to only consider about 200 nodes in the first iteration for our algorithm. The segmentation result given by our proposed algorithm, where only around ten homogeneous regions with similar regular patterns inside are left. This fact demonstrates that the segmentation results are indeed the effects of our proposed algorithm rather than the superpixel generation algorithm.

B. Choice of Color Space

To capture dissimilar characteristics of the color, various color spaces are proposed in³², such as RGB, L * a * b, YUV, HSV, and XYZ. To achieve good segmentation performance,

Algorithm 1 Modularity-Based Image Segmentation

Input: Given a color image I and its oversegmented initialization with a set of superpixels $R = \{R_1, \dots, R_n\}$

- 1: while Pixel labels still change do
- 2: Reconstruct the neighborhood system for each region in R.
- 3: Recompute the HoS texture feature and estimate the distribution of the color feature for each region.
- 4: Adaptively update the similarity matrix W according to Equation (10), $W_{ij} \neq 0$ only if R_i and R_j are adjacent regions in .
- 5: while modularity increase still exists by merging any two adjacent regions do
- 6: for each region $R_i \in R$ do

7: Compute the modularity increase caused by merging region R_i with any of its neighboring regions according to (4) and find the neighboring region R_j , which gives the largest modularity increase among all of the neighboring regions of R_i .
8: Merge regions R_i and R_j by setting the labels of pixels in these two regions to be of the same label
9: end for
10: end while
11: Update the region labels to get a new set of regions $R = \{R_1, \dots, R_m\}$, where m is current number of regions;
12: end while
Output: The set of image segments R .

The select of color space is very significant. Among all the color spaces, the $L * a * b$ color space is identified to be in accord with human visual system and perceptually uniform; hence the image representation in this color space has been widely used in the field of image processing and computer vision. Because of this facet, all of our considerations of the algorithm are in the $L * a * b$ color space. Later, in the experimental calculation section, we have also validated that the segmentation performance in $L * a * b$ color space is much better than that in the RGB color space.

C. Neighborhood System Construction

Dissimilar from normal networks, such as social networks or citation networks, images have self-contained spatial a priori information, that is, spatial coherent regions are more expected to be observed as a single segment, while regions far away from each other are more likely to go to different segments. Hence, different from Louvain method where two regions are deliberated to be neighbors as long as the similarity weight between them are nonzero, we have as an alternative constructed a different neighborhood system by incorporating this spatial a earlier information of images. To be definite, we only consider the possibility of merging neighboring regions in the image all through each aggregation method. To accomplish this, for each region in the image, we only contemplate the adjacent regions of this region to be its neighbors and accumulation its neighboring regions using an adjacent list. The adjacent regions are defined to be the regions that share at least one pixel with the current region. In the following methods for the likeness matrix construction and aggregation, we only consider the current region and the regions in its neighborhood system.

D. Features for Similarity

Color is the most straightforward and important feature for segmentation, so we use the pixel value in the $L * a * b$ color space as one of the features for computing the similarity. However, the color feature alone cannot achieve good segmentation performance, because it does not consider the repetitive patterns of different colors in some homogeneous object. The black and white stripe regularities on zebra would be treated as a whole part according to

human's perception. Simply using color feature will break down these regularities into different segments. To address this problem, we not only employ the color feature, but we have also proposed a novel texture feature to capture the regularities in the image. Our proposed texture depicter is motivated by the histogram of oriented gradients (*HOG*)¹ for pedestrian detection; however, instead of constructing a histogram of gradients.

3. EXPERIMENTS

Full results present three measures. The optimal image scale (OIS) is the F-Measure score obtained using the optimal threshold on each image. The last measure is the average precision (AP) and corresponds to the area under the precision-recall curves of Fig. 1. The user manually defines a rough contour and the algorithm aims at extracting an accurate contour path from it. First, all the pixels that do not belong to the rough contour are considered forbidden. Then, taking advantage of the user interaction, we consider that the rough contour path is ordered and follows the true contour. Thus, intermediate control points regions are automatically spread at regular intervals within the rough contour. Using the rough contour tool has several advantages.

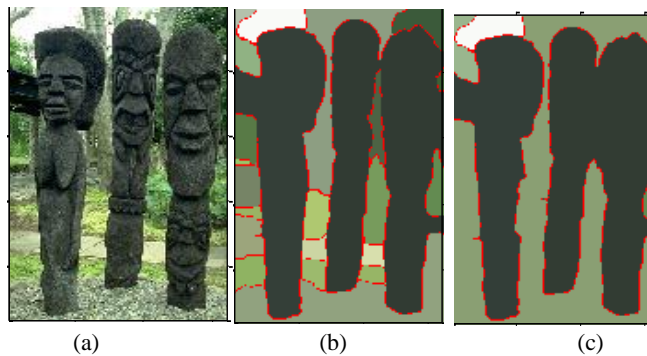


Fig. 1. Image segmentation results (a) previous method (b) proposed method for the stone image

First, the extraction process is efficient since the space problem is constrained. Second, it is certainly more convenient for the user since, unlike the first two tools that often result in a trial-and-error procedure; this one only needs one simple fast interaction.



Fig. 2. Image segmentation results (a) previous method (b) proposed method for the man image

4. PERFORMANCE PARAMETER

We also calculate the performance using the standard boundary-based methodology established in¹. This structure first gets the optimal boundary corresponding between the testing segmentation and the ground-truth, and then calculates the results from two phases: Precision and Recall. Given the testing segmentation C_{test} and the ground truth segmentation C_{gt} , the Precision measures the fraction of identified boundary pixels that match the ground-truth boundaries, and is well-defined as

$$\text{Precision} = \frac{|C_{\text{test}} \cap C_{\text{gt}}|}{|C_{\text{test}}|} \quad (12)$$

Where $|C|$ is the number of boundary pixels in the segmentation C . Similarly, the Recall is defined as

$$\text{Recall} = \frac{|C_{\text{test}} \cap C_{\text{gt}}|}{|C_{\text{gt}}|} \quad (13)$$

Which measures the fraction of ground-truth boundary pixels that are detected. To encapsulate these two indexes, the global F_α -measure, defined in (14), is used to measure the harmonic mean of the Precision and Recall. We set $\alpha = 0.5$ and use it for all the experiments

$$F_\alpha = \frac{\text{Precision} \cdot \text{Recall}}{(1 - \alpha) \cdot \text{Recall} + \alpha \cdot \text{Precision}} \quad (14)$$

Table 1 lists the Precision and Recall values for different algorithms under the same settings as the region level evaluation. The comparison parameters in which the precision is improved recall rate is approx. same.

Table 1 the precision recall and f-measure parameter comparison for baseline and proposed method

Images	Methods	Precision	Recall	F_α Measure
Stone Image	Previous Method	0.733	0.508	0.60
	Proposed Method	0.785	0.505	0.63
Man Image	Previous Method	0.813	0.518	0.61
	Proposed Method	0.819	0.512	0.62

CONCLUSIONS

This paper shows an efficient image contour detection algorithm taking advantages of the scalability of modularity optimization and the inherent properties of images. Adopting the bottom-up framework, the proposed algorithm automatically detects the number of segments in the image, and by employing the color feature as well as the proposed HoS texture feature; it adaptively constructs the similarity matrix among different regions, optimizes the modularity, and aggregates the neighboring regions iteratively. The optimal contour detection is achieved when no modularity increase by neighboring regions aggregation. Results of extensive experiments have validated that the proposed algorithm gives impressive qualitative contour detection results. In upcoming, the more refined design of region/contour cues could benefit to extract contours of complex objects.

REFERENCES

1. S. Li and D. Oliver Wu “Modularity-Based Image Segmentation” *IEEE Transactions on Circuits And Systems For Video Technology*, Vol. 25, No. 4, April (2015).
2. B. Bhanu and J. Peng, “Adaptive integrated image segmentation and object recognition,” *IEEE Trans. Syst., Man, Cybern. C, Appl. Rev.*, vol. 30, no. 4, pp. 427–441, Nov. (2000).
3. J. Shi and J. Malik, “Normalized cuts and image segmentation,” *IEEE Trans. Pattern Anal. Mach. Intell.*, vol. 22, no. 8, pp. 888–905, Aug. (2000).
4. D. Comaniciu and P. Meer, “Mean shift: A robust approach toward feature space analysis,” *IEEE Trans. Pattern Anal. Mach. Intell.*, vol. 24, no. 5, pp. 603–619, May (2002).
5. P. Felzenszwalb and D. Huttenlocher, “Efficient graph-based image segmentation,” *Int. J. Comput. Vis.*, vol. 59, no. 2, pp. 167–181, (2004).
6. P. Arbeláez, M. Maire, C. Fowlkes, and J. Malik, “From contours to regions: An empirical evaluation,” in *Proc. IEEE Conf. Comput. Vis. Pattern Recognit. (CVPR)*, pp. 2294–2301 Jun. (2009).
7. S. Rao, H. Mobahi, A. Yang, S. Sastry, and Y. Ma, “Natural image segmentation with adaptive texture and boundary encoding,” in *Proc. Asian Conf. Comput. Vis. (ACCV)*, pp. 135–146 (2010).
8. P. Arbelaez, M. Maire, C. Fowlkes, and J. Malik, “Contour detection and hierarchical image segmentation,” *IEEE Trans. Pattern Anal. Mach. Intell.*, vol. 33, no. 5, pp. 898–916, May (2011).
9. H. Zhu, J. Zheng, J. Cai, and N. M. Thalmann, “Object-level image segmentation using low level cues,” *IEEE Trans. Image Process.*, vol. 22, no. 10, pp. 4019–4027, Oct. (2013).
10. M. Wertheimer, “Laws of organization in perceptual forms,” in *A Source Book of Gestalt Psychology*. Evanston, IL, USA: Routledge, pp. 71–88 (1938).
11. D. D. Hoffman and M. Singh, “Saliency of visual parts,” *Cognition*, vol. 63, no. 1, pp. 29–78, (1997).
12. T. Cour, F. Benezit, and J. Shi, “Spectral segmentation with multiscale graph decomposition,” in *Proc. IEEE Conf. Comput. Vis. Pattern Recognit. (CVPR)*, vol. 2. pp. 1124–1131 Jun. (2005).
13. J. Wang, Y. Jia, X.-S. Hua, C. Zhang, and L. Quan, “Normalized tree partitioning for image segmentation,” in *Proc. IEEE Conf. Comput. Vis. Pattern Recognit. (CVPR)*, pp. 1–8 Jun. (2008).
14. C. Couprie, L. Grady, L. Najman, and H. Talbot, “Power watershed: A unifying graph-based optimization framework,” *IEEE Trans. Pattern Anal. Mach. Intell.*, vol. 33, no. 7, pp. 1384–1399, Jul. (2011).
15. L. Vincent and P. Soille, “Watersheds in digital spaces: An efficient algorithm based on immersion simulations,” *IEEE Trans. Pattern Anal. Mach. Intell.*, vol. 13, no. 6, pp. 583–598, Jun. (1991).
16. V. Grau, A. U. Mewes, M. Alcaniz, R. Kikinis, and S. K. Warfield, “Improved watershed transform for medical image segmentation using prior information,” *IEEE Trans. Med. Imag.*, vol. 23, no. 4, pp. 447–458, Apr. (2004).

17. X. C. Tai, E. Hodneland, J. Weickert, N. V. Bukoreshtliev, A. Lundervold, and H.H. Gerdes, "Level set methods for watershed image segmentation," in *Scale Space and Variational Methods in Computer Vision*. Berlin, Germany: Springer-Verlag, pp. 178–190 (2007).
18. V. Osmá-Ruiz, J. I. G. Llorente, N. S. Lechón, and P. Gómez-Vilda, "An improved watershed algorithm based on efficient computation of shortest paths," *Pattern Recognit.*, vol. 40, no. 3, pp. 1078–1090, (2007).
19. G. Mori, "Guiding model search using segmentation," in *Proc. 10th IEEE Int. Conf. Comput. Vis. (ICCV)*, vol. 2, pp. 1417–1423, Oct. (2005).
20. K. N. Plataniotis and A. N. Venetsanopoulos, *Color Image Processing and Applications*. New York, NY, USA: Springer-Verlag, (2000).
21. D. Martin, C. Fowlkes, D. Tal, and J. Malik, "A database of human segmented natural images and its application to evaluating segmentation algorithms and measuring ecological statistics," in *Proc. 8th IEEE Int. Conf. Comput. Vis. (ICCV)*, vol. 2, pp. 416–423, Jul. (2001).
22. Y. Kurmi and V. Chaurasia, "An image fusion approach based on adaptive fuzzy logic model with local level processing," *Int. Jour. of Comp. Appl.*, vol. 124, no.1, pp. 39-42, Aug. (2015).
23. S. Tiwari, K. Chauhan, and Y. Kurmi "Shadow detection and compensation in aerial images using MATLAB," *Int. Jour. of Comp. Appl.*, vol. 119, no.20, pp. 5-9, June (2015).
24. Y. Kurmi and V. Chaurasia, "Performance of haze removal filter for hazy and noisy images," *Int. Jour. of Sci. Engg. and Tech.*, vol. 3 no. 4, pp. 437-439 Apr. (2014).
25. M. K. Patle, B. Chourasia, and Y. Kurmi, "High Dynamic Range Image Analysis through Various Tone Mapping Techniques," *Int. Jour. of Comp. Appl.*, vol.153, no.11, pp.14-17, Nov. (2016).
26. A. Kumar, B. Chourasia, and Y. Kurmi, "Image defogging by multiscale depth fusion and hybrid scattering model," *International Journal of Computer Applications* (0975 – 8887), vol. 155, no 11, pp. 34-38, Dec. (2016).
27. D. Swami, B. Chaurasia and Y. Kurmi, "A Multiscale Particle Filter and Multi-Feature Based Contour Detection," *International Journal of Advanced Engineering and Management*, Vol. 2, No. 6, pp. 127-131, (2017).
28. N. Dhaware, B. Chaurasia and Y. Kurmi, "Analysis of Image Quality Enhancement Using Colour Depth Histogram and Luminance Contrast Masking," *International Journal of Advanced Engineering and Management*, Vol. 2, No. 5, pp. 109-112, (2017).
29. K. Zhang, Q Liu, H. Song, and X. Li, "A Variational Approach to Simultaneous Image Segmentation and Bias Correction," *IEEE Transactions on Cybernetics*, vol. 45, no. 8, pp. 1426-1437, August (2015).
30. K. Zhang, L. Zhang, K. M. Lam, and David Zhang, "A Level Set Approach to Image Segmentation with Intensity Inhomogeneity," *IEEE Trans. on Cybernetics*, vol. 46, No. 2, pp.546-557, Feb. (2016).
31. M. Wang, J. Huang, and D. Ming, "Region-Line Association Constraints for High-Resolution Image Segmentation," *IEEE Journal of Selected Topics in Applied Earth Observations and Remote Sensing*, Vol. 10, No. 2, pp.628-637, Jan. (2017).
32. S. Dev, Yee H. Lee, and S. Winkler, "Color-Based Segmentation of Sky/Cloud Images From Ground-Based Cameras," *IEEE Journal of Selected Topics in Applied Earth Observations and Remote Sensing*, Vol. 10, No. 1, pp.231-242, Jan. (2017).